

Compare Linear Interpolation and Adaptive Smoothing Methods on Traffic Flow Information Reconstruction

Wei Guo, Qi Wang, Zhiheng Li, Jiyan Tan, Yi Zhang, Li Li, Zuo Zhang

Abstract—With rapid development of transportation system, traffic information collection, which provides accurate and reliable traffic data, receives more and more attentions. However, under practical conditions, most roads and freeways are equipped with limited amount of loop detectors. Thus, researchers are delving into traffic information reconstruction by utilizing limited information. In this paper, we compare the classical linear interpolation method and a special nonlinear interpolation method, the adaptive smoothing method, on reconstructing the spatial-temporal dynamics of traffic flow rate, density and velocity. Tests on NGSIM dataset show that both methods are effective.

I. INTRODUCTION

Traffic information collection provides essential traffic data for Intelligent Transportation Systems (ITS). Research on traffic flow measuring [1], travel time estimation [2], traffic status recognition [3] relies on the accuracy and reliability of collected traffic data.

In practice, traffic data can be collected from different kinds of sensors. These sensors can be divided into two classes: fixed sensors and moving probes. On one hand, traffic information are often acquired by inductive loop detectors, microwave radars, active inferred detectors, ultrasonic sensors and video cameras arranged at a specific position of the road [4]. On the other hand, probe vehicles move along the road networks to gather the floating car data (FCD), aggregating them to traffic information center (TIC) through wireless communication. Advanced study has involved in the fusion of diverse traffic data from dissimilar traffic detectors [5].

Constrained by financial budgets, lots of roads and freeways are merely equipped with inductive loop detectors. So, it is still important to discuss how to reconstruct the spatial-temporal traffic information based on the settled loop sensor data.

Considering the cost of laying the detector, we expect to exploit traffic dynamics with limited detectors and obtain section traffic flow information as accurate as possible. Interpolation, as an efficient tool in numerical analysis, is most frequently mentioned method for such propose. Triber and Helbing [6] put forward another reconstruction method that was named “adaptive smoothing”, aiming at acquisition of spatial-temporal traffic situations. A detailed introduction about these two methods would be launched in the following section.

In this paper, we would like to compare the performance of linear interpolation method and adaptive smoothing method based on NGSIM dataset tests. As a result, we expect a reference to guide us rationally choosing the reconstruction method.

The rest of paper was organized as follows. *Section II* reviews the linear interpolation and adaptive smoothing methods and how we practically apply and compare them. In *Section III*, we introduce evaluation criteria of reconstruction performance, whose detailed expressions are given in *Part A*. Then, *Part B* shows the application to Interstate 80 Freeway under the circumstances of different sensor layout intervals. Conclusions are made and discussed in *Section IV* ultimately.

II. REVIEW OF LINEAR INTERPOLATION AND ADAPTIVE SMOOTHING METHODS

Before reviewing the reconstruction methods, let us first recall the objective of reconstructing work.

Suppose there is a certain number of detectors distributed along the freeways, we could attain limited traffic information of fracture surface. In general, we use trajectory to denote a vehicle’s movement. Trajectory is a kind of two dimensional curve formed by time and position (t, x) . If we add a new parameter v that indicates the vehicle velocity at trajectory point (t, x) , the trajectory curve extends to a three dimensional surface, which can reflect the spatial-temporal traffic information. Therefore, the algorithm we describe in the following is to recur to the complete spatial-temporal traffic information surface via incomplete traffic data.

Next, we introduce the typical and widely recognized method, interpolation method. The interpolation method contains nonlinear interpolation and linear interpolation methods. Nonlinear interpolation methods are great at calculative precision. However, any increase or decrease on interpolation nodes lead to the modification of whole interpolation base functions. On the contrary, linear interpolation algorithm has a simple and concise maneuverability and yet it is effective. Thus, we choose linear interpolation algorithm to apply to our test.

Manuscript received March 15th, 2012.

W. Guo is with Department of Automation, Tsinghua University, Beijing, China 100084. (e-mail: guo-w11@mails.tsinghua.edu.cn).

Q. Wang was once with Department of Automation, Tsinghua University, Beijing, China 100084. (e-mail: qi-wang06@mails.tsinghua.edu.cn).

Z. Li is with Department of Automation, TNLi, Tsinghua University, Beijing, China 100084. (e-mail: zhli@mail.tsinghua.edu.cn).

J. Tan is with Department of Automation, Tsinghua University, Beijing, China 100084. (e-mail: tjyphilip@163.com).

Y. Zhang is with Department of Automation, TNLi, Tsinghua University, Beijing, China 100084. (e-mail: zhyi@mail.tsinghua.edu.cn).

L. Li is with Department of Automation, TNLi, Tsinghua University, Beijing, China 100084 (corresponding author, phone: +86 (10) 62782071; e-mail: li-li@mail.tsinghua.edu.cn).

Z. Zhang is with Department of Automation, TNLi, Tsinghua University, Beijing, China 100084. (e-mail: zhangzuo@mail.tsinghua.edu.cn).

Previous literatures e.g. [7] presented three common linear interpolation methods for velocity evolution pattern reconstruction. Figure 1 illustrates the detailed arithmetic for these methods. Several detectors are equidistantly configured along the freeways. We nominated them as **a**, **b**, **c**, **d** in order.

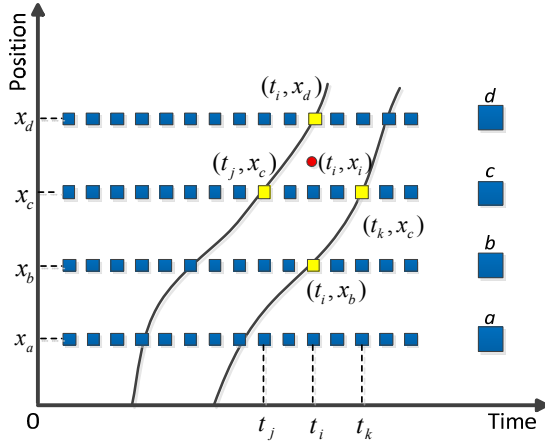


Figure 1 The graphical representation of linear interpolation

1. Nearest Spatial Neighboring Points Interpolation

In this method, the target value is interpolated by the most adjacent detector points. The mathematic expression is

$$v(t_i, x_i) = v(t_i, x_d) \quad (1)$$

2. Nearest Temporal Neighboring Points Interpolation

Distinct from the above, we interpolate the objective value by utilizing the contiguous traffic data that sampled at the same time. So we get

$$v(t_i, x_i) = \frac{w_b v(t_i, x_b) + w_d v(t_i, x_d)}{w_b + w_d} \quad (2)$$

3. Nearest Spatial-Temporal Neighboring Points Interpolation

Interpolate the target value by N adjoining detector points. We take $N = 4$ as example.

$$v(t_i, x_i) = \frac{w_b v(t_i, x_b) + w_c v(t_j, x_c) + w_{c'} v(t_k, x_c) + w_d v(t_i, x_d)}{w_b + w_c + w_{c'} + w_d} \quad (3)$$

The above expression seems more complex, it in fact can be viewed as generalization of Nearest Temporal Neighboring Points Interpolation method. The weighting factors $w_b, w_c, w_{c'}, w_d$ are defined as the inverse distance.

$$w_b = \frac{1}{\sqrt{(t_i - t_j)^2 + \sqrt{(x_i - x_b)^2}}} = \frac{1}{|x_i - x_b|} \quad w_c = \frac{1}{\sqrt{(t_i - t_j)^2 + \sqrt{(x_i - x_c)^2}}}$$

$$w_{c'} = \frac{1}{\sqrt{(t_i - t_k)^2 + \sqrt{(x_i - x_c)^2}}} \quad w_d = \frac{1}{\sqrt{(t_i - t_i)^2 + \sqrt{(x_i - x_d)^2}}} = \frac{1}{|x_i - x_d|}$$

Compared to the directly perceived processing method above, Triber and Helbing [6] introduce a nonlinear low-pass filter to smooth the traffic data of fixed detector sensors. The method partially incorporates *a priori* knowledge, traffic flow information and involves in two kinds of typical traffic situations, free-flow traffic status and congested traffic status.

Eq. (4) expresses the weighted superposition of congested traffic and free traffic as follows.

$$y(x, t) = w(y_{cong}, y_{free}) y_{cong}(x, t) + [1 - w(y_{cong}, y_{free})] y_{free}(x, t) \quad (4)$$

where $y(x, t)$ denotes the quantity of traffic data at the point (x, t) . Furthermore, we will discuss how to calculate the weighting items and quantities.

According to empirical knowledge, perturbations of velocity propagate along the direction of traffic flow at a nearly constant velocity c_{free} in condition of free-flow traffic. Whereas, perturbations move against the congested traffic flow with another invariant velocity c_{cong} . Hence, the filter should be available to accept those perturbations with c_{free} and c_{cong} transmitting velocity, respectively. Meanwhile, the high frequency or spatial components, viewed as fluctuations, should be filtered out.

Before putting forward the filter, we should discretize the variables of t and x . As the illustration in Figure 2, the stationary detectors are placed equidistantly along the freeways, which forms a rectangular grid with the range of $x \in [x_{min}, x_{max}]$ and $t \in [t_{min}, t_{max}]$. Set two parameters Δx and Δt for the spatial-temporal resolution. $\Delta x, \Delta t$ denotes the position intervals and time aggregation intervals defined as follows.

$$\Delta x = x_\alpha - x_{\alpha-1} \quad (5)$$

$$\Delta t = t_\beta - t_{\beta-1} \quad (6)$$

where α and β are index coefficients.

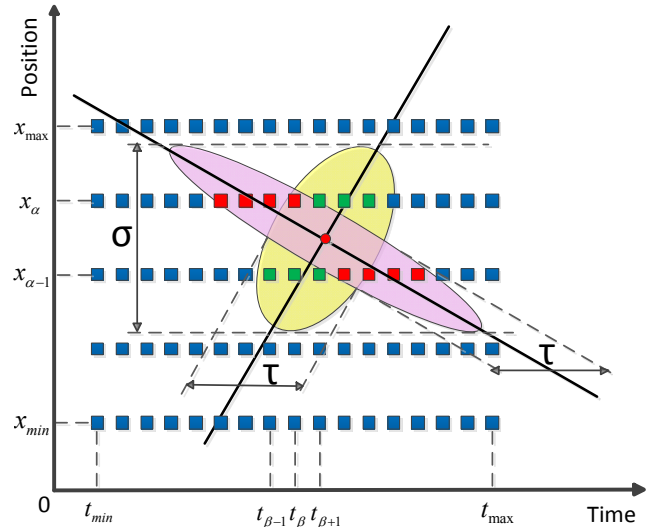


Figure 2 Visualization of influence area of the anisotropic filter

Based on the above-mentioned discussion, we introduce the anisotropic filter.

$$y_{cong}(x, t) = \frac{1}{U_{cong}(x, t)} \sum_{\alpha=\alpha_{min}}^{\alpha_{max}} \sum_{\beta=\beta_{min}}^{\beta_{max}} \psi_{cong}(x_\alpha - x, t_\beta - t) y_{\alpha\beta} \quad (7)$$

$$y_{free}(x, t) = \frac{1}{U_{free}(x, t)} \sum_{\alpha=\alpha_{min}}^{\alpha_{max}} \sum_{\beta=\beta_{min}}^{\beta_{max}} \psi_{free}(x_{\alpha} - x, t_{\beta} - t) y_{\alpha\beta} \quad (8)$$

with $x_{\alpha} = x_{min} + \alpha\Delta x$ and $t_{\beta} = t_{min} + \beta\Delta t$. The normalization function, $U_{free}(x, t)$ and $U_{cong}(x, t)$, guarantee the equivalent relations between the input data and output data. They are defined in the following expressions (9) and (10).

$$U_{cong}(x, t) = \sum_{\alpha=\alpha_{min}}^{\alpha_{max}} \sum_{\beta=\beta_{min}}^{\beta_{max}} \psi_{cong}(x_{\alpha} - x, t_{\beta} - t) \quad (9)$$

$$U_{free}(x, t) = \sum_{\alpha=\alpha_{min}}^{\alpha_{max}} \sum_{\beta=\beta_{min}}^{\beta_{max}} \psi_{free}(x_{\alpha} - x, t_{\beta} - t) \quad (10)$$

As regards to the filter kernel, Triber and Helbing [6] turned out that negative exponential function had feasible and favorable performance in their application to German Freeways.

Eq. (11) describes the form of kernel function.

$$\psi_0(x, t) = e^{-\frac{|x|}{\sigma} - \frac{|t|}{\tau}} \quad (11)$$

which indicates the kernel function depends on both position and time, σ and τ describe the converge area around the point (x, t) with the quantity $y(x, t)$ to be estimated. After coordinate transformation, we obtain the two kinds of anisotropic filter kernels.

$$\psi_{cong}(x, t) = \psi_0(x, t - \frac{x}{c_{cong}}) \quad (12)$$

$$\psi_{free}(x, t) = \psi_0(x, t - \frac{x}{c_{free}}) \quad (13)$$

At last, we deal with the remainder items, weighting items. Triber and Helbing [6] propose to exploit the velocity data $u(x, t)$ and hyperbolic tangent function to compute the factor by the following equation.

$$\begin{aligned} w(y_{cong}, y_{free}) &= w(u_{cong}(x, t), u_{free}(x, t)) \\ &= \frac{1}{2} [1 + \tanh(\frac{u_c - u^*(x, t)}{\Delta u})] \end{aligned} \quad (14)$$

where $u^*(x, t) = \min(u_{cong}(x, t), u_{free}(x, t))$.

To sum up, Eq. (4) describe the adaptive smoothing method. The involved parameters of the anisotropic filters, kernel functions and weighted factors are given in Eq. (7)-(8), (12)-(14).

III. TEST AND DISCUSSION

In this section, we firstly introduce the evaluation criteria of traffic information reconstruction. Then, we present the tests results based on NGSIM dataset.

A. Evaluation Criteria of Traffic Information Reconstruction

In this article, we adopt the following four kinds of reconstruction error criteria to evaluate the reconstruction performance. We take velocity reconstruction for example.

1. Root Mean Square Error (RMSE)

$$E(RMSE) = \sqrt{\frac{\sum_{\alpha=0}^{M-1} \sum_{\beta=0}^{N-1} (v_{\alpha\beta}(x_{\alpha}, t_{\beta}) - \hat{v}_{\alpha\beta}(x_{\alpha}, t_{\beta}))^2}{M \times N}} \quad (15)$$

2. Relative Root Mean Square Error (RRMSE)

$$E(RRMSE) = \sqrt{\frac{\sum_{\alpha=0}^{M-1} \sum_{\beta=0}^{N-1} \frac{(v_{\alpha\beta}(x_{\alpha}, t_{\beta}) - \hat{v}_{\alpha\beta}(x_{\alpha}, t_{\beta}))^2}{v_{\alpha\beta}(x_{\alpha}, t_{\beta})}}{M \times N}} \quad (16)$$

3. Mean Absolute Deviation (MAD)

$$E(MAD) = \sqrt{\frac{\sum_{\alpha=0}^{M-1} \sum_{\beta=0}^{N-1} |v_{\alpha\beta}(x_{\alpha}, t_{\beta}) - \hat{v}_{\alpha\beta}(x_{\alpha}, t_{\beta})|}{M \times N}} \quad (17)$$

4. Relative Mean Absolute Deviation (RMAD)

$$E(RMAD) = \sqrt{\frac{\sum_{\alpha=0}^{M-1} \sum_{\beta=0}^{N-1} \frac{|v_{\alpha\beta}(x_{\alpha}, t_{\beta}) - \hat{v}_{\alpha\beta}(x_{\alpha}, t_{\beta})|}{v_{\alpha\beta}(x_{\alpha}, t_{\beta})}}{M \times N}} \quad (18)$$

where $t_{\alpha} = t_{min} + \alpha\Delta t$, $x_{\beta} = x_{min} + \beta\Delta x$,

$$M = \frac{t_{max} - t_{min}}{\Delta t} + 1, \quad N = \frac{x_{max} - x_{min}}{\Delta x} + 1$$

$v_{\alpha\beta}(x_{\alpha}, t_{\beta})$ stands for the true value of velocity at (x_{α}, t_{β}) , $\hat{v}_{\alpha\beta}(x_{\alpha}, t_{\beta})$ stands for the reconstructed value of velocity at (x_{α}, t_{β}) .

B. Tests and Discussions Based on NGSIM Dataset

In this section, we present the test settings and the detailed implementation of the above reconstruction algorithms. Visualized figures of test results, as well as correlative analysis and discussion, will also be listed in this part.

We make use of Next Generation Simulation (NGSIM) dataset [12] to test and verify the linear interpolation and adaptive smoothing methods. Thanks to its high accuracy and great reliability, more and more researchers prefer to do research based on NGSIM dataset. Therefore, the wide recognition and acceptability of NGSIM dataset is undoubted.

We use the data of I80 and I101 Expressway. I80 dataset is constituted by the data of three time segments: 4:00pm-4:15pm, 5:00pm-5:15pm, 5:15pm-5:30pm. Similarly, I101 dataset is also constituted by the data of three time segments: 7:50am-8:05am, 8:05am-8:20am, 8:20am-8:35am. Figure 3 shows us the diagrammatic drawing for I80 Freeway, which is similar to the configuration for I101 Freeway. Since the auxiliary lane (lane 6 in Figure 3) is vulnerable to the variation of traffic flow in on or off ramp areas, we restrict our study area into lane 1 to lane 5.

In our test, we set the equidistant virtual loop detectors distributed along the road, which has been shown in Figure 3. Limited by the paper length, we take detector layout of I80 Freeway for example.

To study the reconstruction errors during the different quantity of traffic detection information, we adjust the distance of spatial intervals of detectors configuration. In other words, detector layout with large spatial intervals means a bit of traffic information, and vice versa.

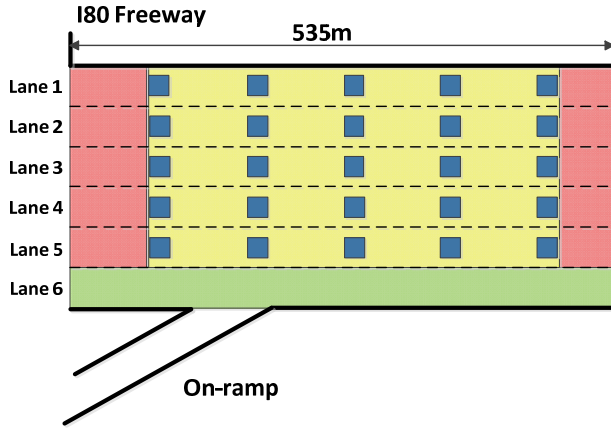


Figure 3 Detector layout of I80 Freeway

Besides, we should point out that in the application of linear interpolation, we adopt Nearest Temporal Neighboring Points Interpolation method within the rectangular grid covered by equidistant positioned detectors. It is marked by the pale yellow area in Figure 3. Considering the carnation area which involves in the region in front of first column

detectors and the region in the rear of last column ones, we utilize the Nearest Spatial Neighboring Interpolation method. That is to say, we think that the quantity of traffic data almost remain invariant at those areas. As for adaptive smoothing method, it can be viewed as another advanced Nearest Spatial-Temporal Neighboring Points Interpolation method. Furthermore, adaptive smoothing method put confirmative empirical knowledge into use. That is also the reason why we get rid of conventional Nearest Spatial-Temporal Neighboring Points Interpolation method in our test.

TABLE I. MEANINGS AND VALUES OF TEST PARAMETERS

Parameters	Meanings	Values
Δx	Spatial resolution	10m
Δt	Temporal resolution	30s
x_{min}	Position of first detector	100m
x_{max}	Position of last detector	500m
t_{min}	Starting time	0s
t_{max}	Termination time	900s
c_{cong}	Speed of propagation in congested traffic	-15km/h
c_{free}	Speed of propagation in free-flow traffic	80km/h
σ	Coefficient of spatial smoothing	0.1km
τ	Coefficient of temporal smoothing	0.5min
u_c	Critical speed between free traffic status to congested traffic status	60km/h
Δu	Breadth of the transition area ¹	20km/h

1. The detailed explanation of this parameter can be seen in Reference [6].

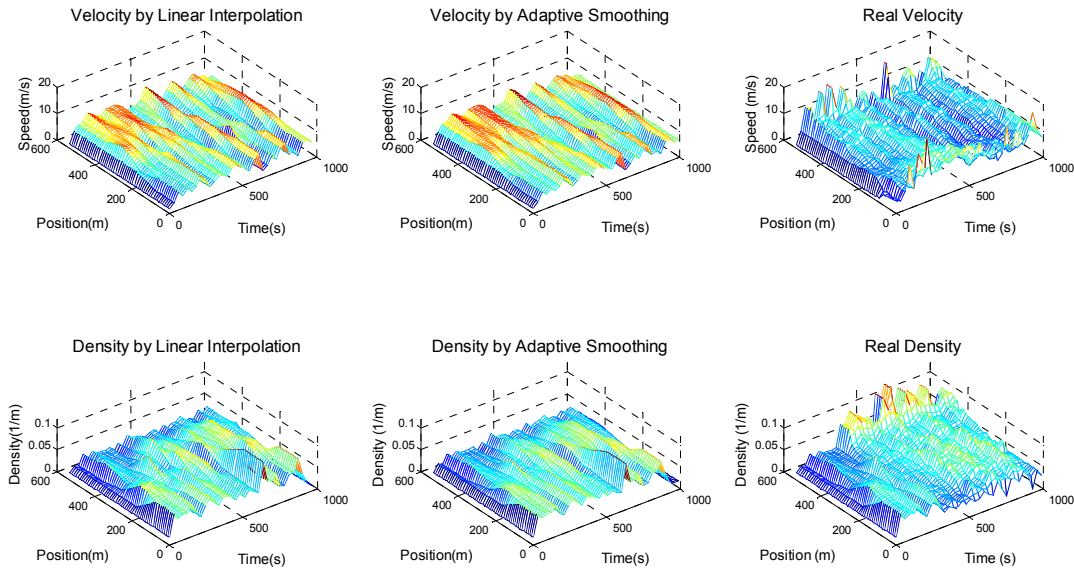


Figure 4 Reconstruction of spatial-temporal velocity and density evolution patterns

Table I lists the meanings and values of those parameters. The values of the parameters for the adaptive smoothing method are chosen according to [6].

We distribute the virtual detectors at intervals of 100m along the lane 1 to lane 5. The starting detectors are localized at 100m while the last ones are localized at 500m. And the spatial-temporal resolution of real velocity and density data is $\Delta t = 0.1s, \Delta x = 10m$.

The reconstruction results of spatial-temporal traffic evolution patterns are visualized in Figure 4. The displayed test results were based on the dataset of I80 during 4:00pm-4:15pm. To make a comparison intuitively, the real spatial-temporal evolution patterns observed by NGSIM are illustrated on the right side of the figure.

To evaluate the reconstruction effect, RMSE, RRMSE, MAD and RMAD errors, demonstrated in *Part A*, would be applied in evaluation criteria. Table II lists the computational values of reconstruction errors. Consistent with the reconstruction test above, we take 100m as the detector intervals.

TABLE II. RECONSTRUCTION ERRORS OF DETECTORS INTERVALS 100M

Errors	Velocity		Density	
	LIM	ASM	LIM	ASM
RMSE	1.0509	1.1150	0.0174	0.0167
RRMSE	0.3004	0.3175	0.2453	0.2347
MAD	0.7808	0.8500	0.0126	0.0122
RMAD	0.1477	0.1576	0.1979	0.1973

As can be seen from Figure 4 and Table II, both the error values of linear interpolation and adaptive smoothing methods are acceptable and tolerable. Figure 5 shows us the velocity

reconstruction results of dataset of I101 7:50am-8:05am, lane 1, which also obtains well effect. All these indicate that spatial-temporal trajectories reconstruction based on linear interpolation and adaptive smoothing methods are practical and efficient.

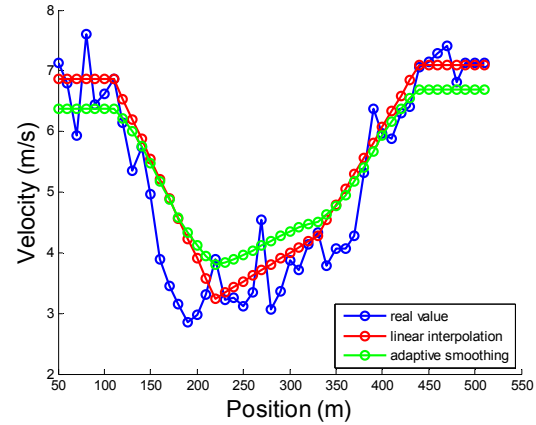


Figure 5 Velocity reconstruction results on dataset of I80, Lane 5

To examine the reconstruction performance, we gradually enlarge the detector intervals from 10m to 210m with an incremental size of 10m. We compare both velocity and density reconstruction. Results indicate that the increasing trend of velocity reconstruction errors is the same as the trend of density reconstruction errors. So, for simplicity, Figure 6 only shows the statistical results of velocity.

We can observe that the smaller the detector intervals are (which means more traffic information is available), the smaller the reconstruction errors are. However, there are several abnormal peaks appear at some specific detector intervals, such as 110m, 140m, 170m.

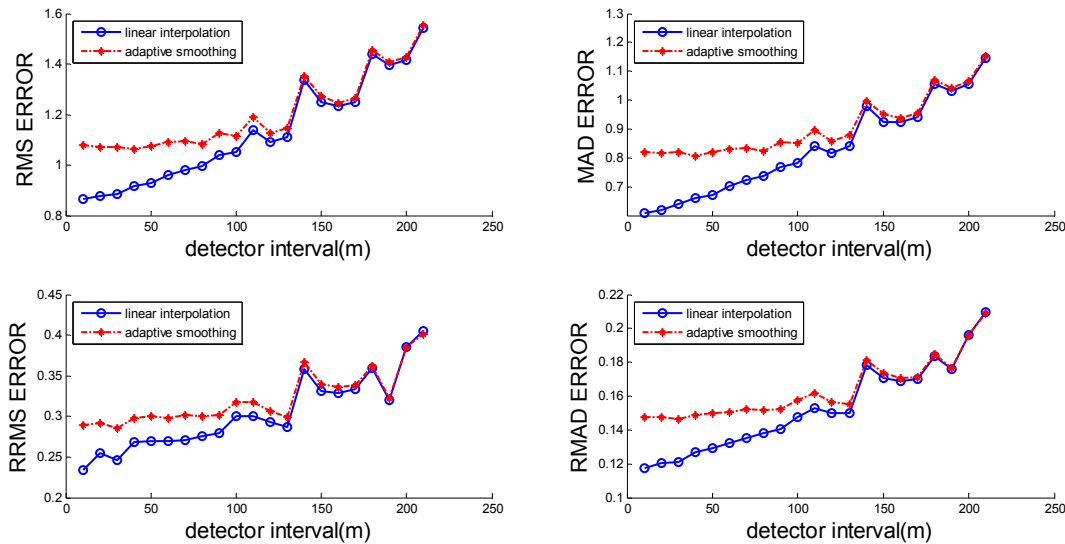


Figure 6 Velocity reconstruction errors under different detector intervals

Both the linear interpolation method and the adaptive smooth method tend to use a smooth curve to approximate the real traffic dynamics. As a result, if some extreme (local maximum or minimum) values of velocity or density are not sampled, the interpolated error at such points would be extraordinary large.

Figure 7 and Figure 8 give two typical reconstruction results, where the detector interval is 110m. The locations of the detectors are labeled out by vertical dash lines. In Figure 7, the sampled values are not the extreme values of the velocities at that time. Neither the linear interpolation nor adaptive smoothing methods show good reconstruction performance. On the contrary, Figure 8 shows the opposite situations. The sampled values are roughly local maximal or minimal of the velocity variation curve. They can reflect the variation tendency of velocity. So, the reconstruction results are good.

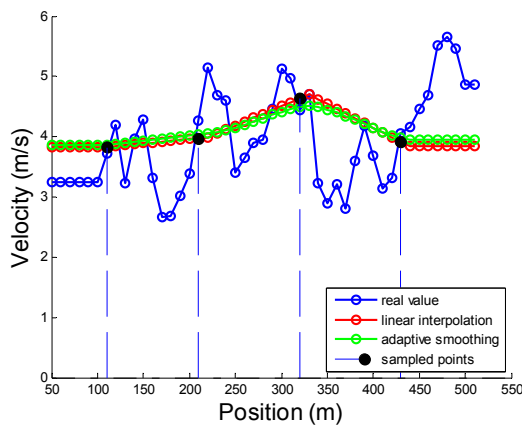


Figure 7 Detector sampled points for I80, Lane 5, 900s

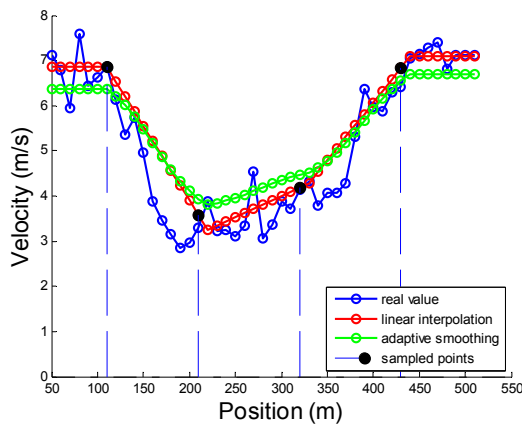


Figure 8 Detector sampled points for I80, Lane 5, 600s

When traffic oscillations occur, there exist a number of extreme value points in the velocity and density curves. The reconstruction errors of linear interpolation method and the adaptive smooth method will be higher than usual.

The detector positions and measure precisions also influence the reconstruction errors, since they determine whether the extreme values of velocity or density could be

sampled. Thus, increasing the temporal measure precisions of detectors is an effective way to eliminate the overlarge errors.

IV. CONCLUSION

This article compares two representative methods: linear interpolation and adaptive smoothing methods, for spatial-temporal traffic information reconstruction based on NGSIM dataset tests. The RMSE, RRMSE, MAD and RMAD errors are adopted to quantitatively evaluate traffic information reconstruction effect. Test results show that

- (1) Linear interpolation method and adaptive smoothing method are both practical and effective algorithms to reconstruct spatial-temporal traffic information.
- (2) The fixed sensors are sometimes unable to capture enough information to reconstruct traffic oscillations. This usually brings extraordinary inaccuracy in traffic flow dynamics reconstruction.

ACKNOWLEDGMENT

This work was supported in part by National Basic Research Program of China (973 Project) 2012CB725405, Hi-Tech Research and Development Program of China (863 Project) 2011AA110301, and National Natural Science Foundation China 60834001, 61021063.

REFERENCES

- [1] Q. Wang, J. Hu, C. Mu, "A method of traffic flow measuring based on infrastructure integration system", *Proceedings of Intelligent Vehicles Symposium*, pp. 945-950, 2009
- [2] J. C. Herrera, A. M. Bayen, "Traffic flow reconstruction using mobile sensors and loop detector data", *Proceedings of 87th Transportation Research Board Annual Meeting*, 2007
- [3] D. Ni, H. Wang, "Trajectory reconstruction for travel time estimation", *Journal of Intelligent Transportation Systems*, vol.12, no.3, pp. 113-125, 2008
- [4] *Traffic Detector Handbook*, Volume I, 3rd edition, US Department of Transportation, Federal Highway Administration, 2006
- [5] J. W. C. van Lint, S. P. Hoogendoorn, "A robust and efficient method for fusing heterogeneous data from traffic sensors on freeways", *Computer-Aided Civil and Infrastructure Engineering*, vol.24, pp.1-17, 2009
- [6] M. Tribler, D. Helbing, "Reconstructing the spatial-temporal traffic dynamics from stationary detector data", *Cooperative Transportation Dynamics*, vol. 1, pp. 3.1-3.24, 2002
- [7] Q. Wang, J. Hu, J. Zhang, Y. Zhang, "Extraction of traffic status based on spatial-temporal trajectory reconstruction", *Proceedings of Transportation of China (AFTC 2010), 6th Advanced Forum*, pp.221-228, 2010
- [8] F. L. Hall, B. N. Persaud, "Evaluation of speed estimates made with single-detector data from freeway traffic management systems", *Transportation Research Record 1232*, pp. 9-16, 1989
- [9] B. S. Kerner, "Theory of breakdown phenomenon at highway bottlenecks", *Transportation Research Record*, vol. 1710, pp. 136-144, 2000
- [10] B. S. Kerner, H. Rehborn, M. Aleksic, A. Haug, "Recognition and tracking of spatial-temporal congested traffic patterns on freeways", *Transportation Research Part C*, vol.12, pp. 369-400
- [11] D. Ichiba, K. Hara, H. Kanoh, "Spatial interpolation of traffic data by genetic fuzzy system", *Proceedings of International Symposium on Evolving Fuzzy Systems*, pp. 280-285, 2006
- [12] Next Generation Simulation (NGSIM) Project: <http://ngsim.fhwa.dot.gov/>